Supplementary Information:

What governs magnetic exchange couplings in radical-bridged dinuclear complexes?

Grégoire David,* Gwenhaël Duplaix-Rata, and Boris Le Guennic

Univ Rennes, CNRS, ISCR (Institut des Sciences Chimiques de Rennes)-UMR 6226,

F-35000 Rennes, France

E-mail: gregoire.david@univ-rennes1.fr

S1 Input file generator

Whilst the methodology to perform the decomposition is relatively simple from the conceptual point of view, its implementation might be more complex since the computation of all contributions of the $\mathcal{N}(\mathcal{N}-1)/2$ couplings requires $2\mathcal{N}(\mathcal{N}-1)/2$ input files. Furthermore, the input files to generate the NO and FC determinants might be tricky to make for having the correct spin distribution and/or relaxations. To ease the use of the method, an automatic input file generator has been developed for the ORCA quantum chemistry package, where the LSCF method to freeze orbitals has been implemented since version 4. This program in Python may be downloaded and is documented on `GitLab` (`https://gitlab.com/gdavid123/input-files-generator`) while its use is shortly summarised here.

The use of this program requires to have previously computed the HS in the RO or QRO formalism and to have localised the SOMOs. To run the program, an input file constituted

of blocks of information must be created. The first block contains general settings while the others define the centres. For the centre blocks, the first line defines the name of the centre and the following gives the MO(s) numbering associated with the centre. All blocks finish by `end`. This results in a file of the following shape, here in the example of a three-centre system (named A, B and C and where the SOMOs go from 181 to 185)

```
input_orca=    # The ORCA input file
loc_orb=       # The gbw file containing the localised orbitals
nbas=          # Number of basis functions
end            # Close the first bloc

A   # First line of centre bloc defines the name use for the directories and input files created
185            # Magnetic orbital localised on the centre A
184            # Magnetic orbital localised on the centre A
end            # close the centre bloc

B   # Start of the second centre
MO 183:   2N  -   0.070011  and   0Ni -   0.798049
# Magnetic orbital localised on the centre B following the ORCA localisation format
MO 182:   1O  -   0.004838  and   0Ni -   0.883228
# Magnetic orbital localised on the centre B following the ORCA localisation format
end            # close the centre bloc

C   # Start of the second centre
181   # Magnetic orbital localised on the centre B
end            # Close the centre bloc
```

The execution of the program creates a folder tree schematised in Figure S1. The first level created corresponds to the NO determinants and the name of the folders are labelled according to the spin distribution : the orbitals are sorted by magnetic centre and ordered according to the folder name. The centres before the underscore are the occupied α magnetic centres, and after the β ones. For instance, the `AC_B` folder would correspond to the $\Phi_{A\bar{B}C,NO}$ determinant. The second level corresponds to the determinants created from the previous BS,NO, i.e. all FC and the FM determinants. For the FC relaxations, the folder is named according to the pair of centres concerned and two files are created, one for the α relaxation and one for the β relaxation. According to the previous example of $\Phi_{A\bar{B}C,NO}$, two pairs might be considered, `A_B` and `C_B`. In the former, two input files would be created, `A_B.alpha.inp` and `A_B.beta.inp`, corresponding to the $\Phi_{A'\bar{B}C,FC}$ and $\Phi_{A\bar{B}'C,FC}$ determinants, respectively.
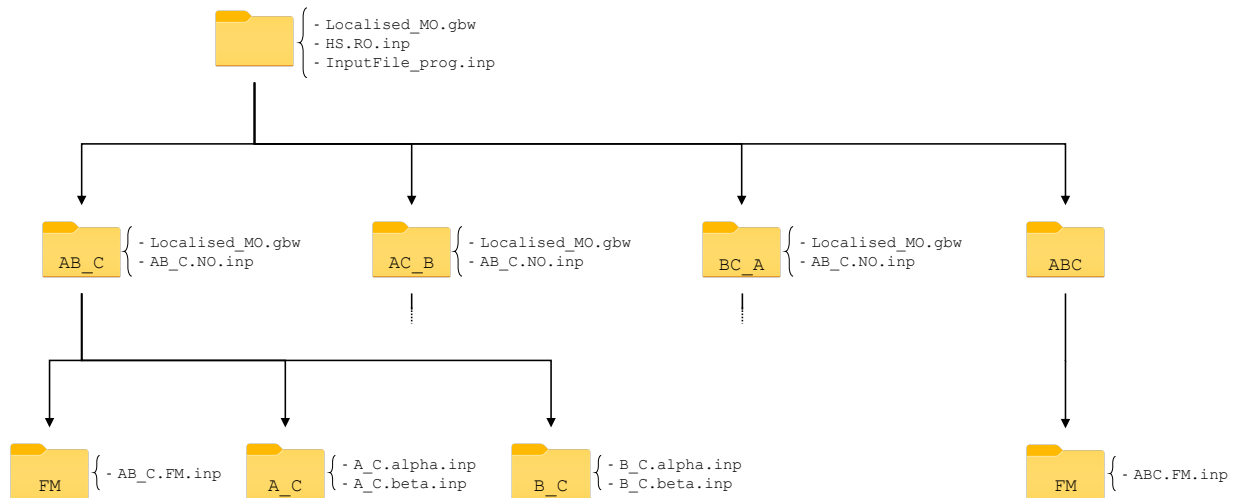
Figure S1: Schematic representation of the folder tree created by the input file generator in a case of three-centre system (with A,B and C).
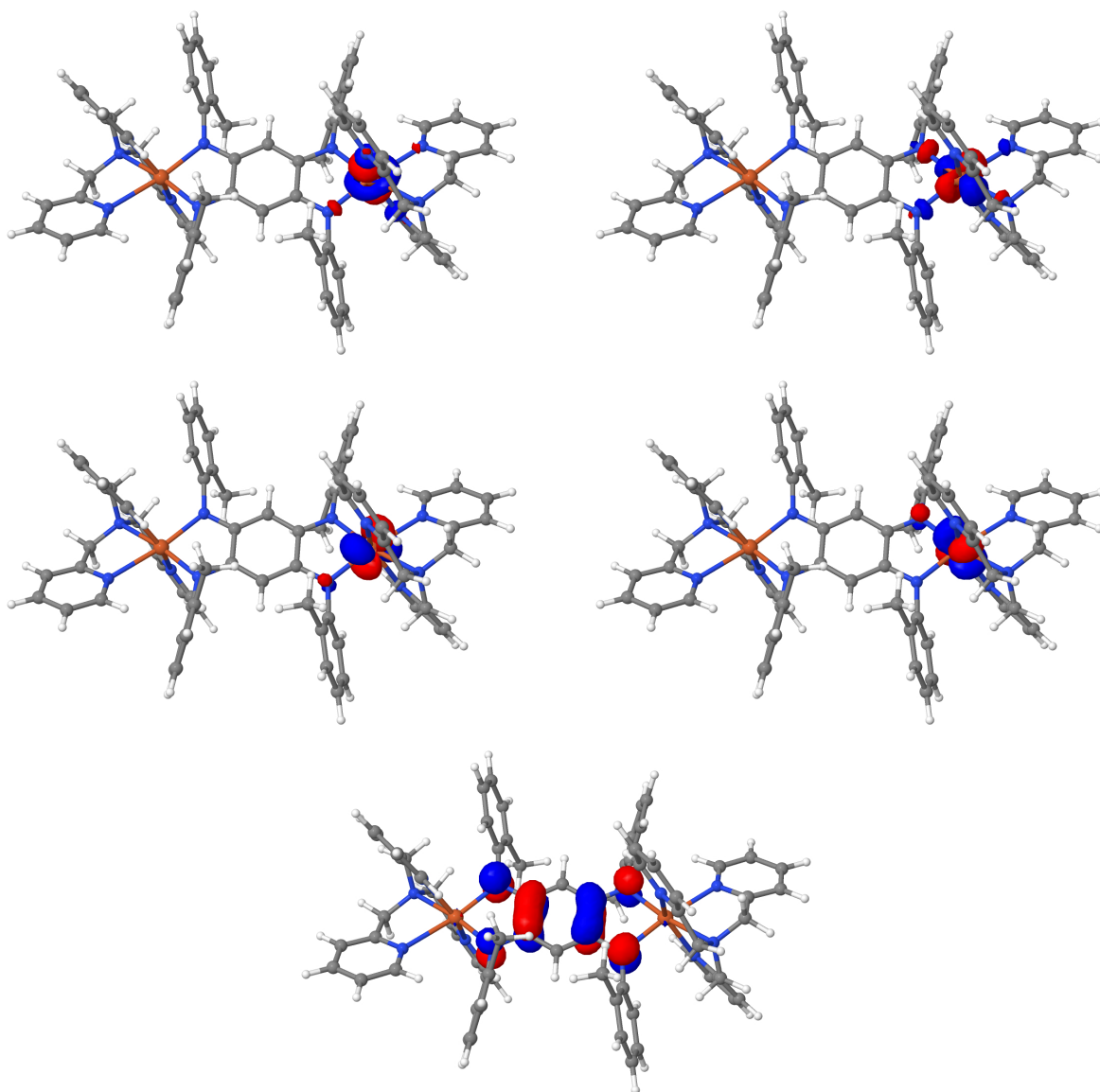
S2   Plots of orbitals

Figure S2: Isosurface of the d_{z^2} (top left), $d_{x^2-y^2}$ (top right), d_{yz} (middle left), d_{xz} (middle right) and π^* radical (bottom) magnetic orbitals of **3a**. Orange = iron, blue = nitrogen, grey = carbon, white = hydrogen. Isovalue = 0.5 a.u..
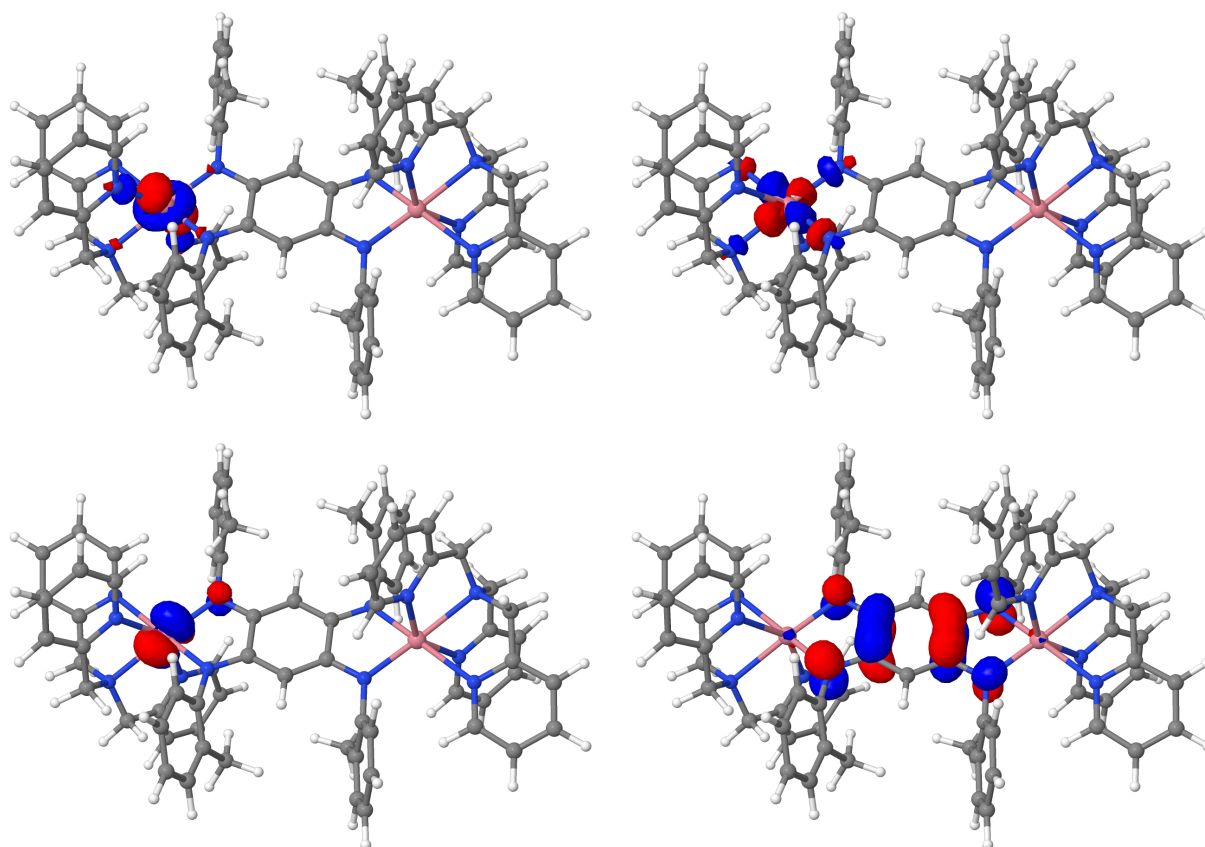
Figure S3: Isosurface of the d_{z^2} (top left), $d_{x^2-y^2}$ (top right), d_{yz} (bottom left) and π^* radical (bottom right) magnetic orbitals of **4a**. Pink = cobalt, blue = nitrogen, grey = carbon, white = hydrogen. Isovalue = 0.5 a.u..
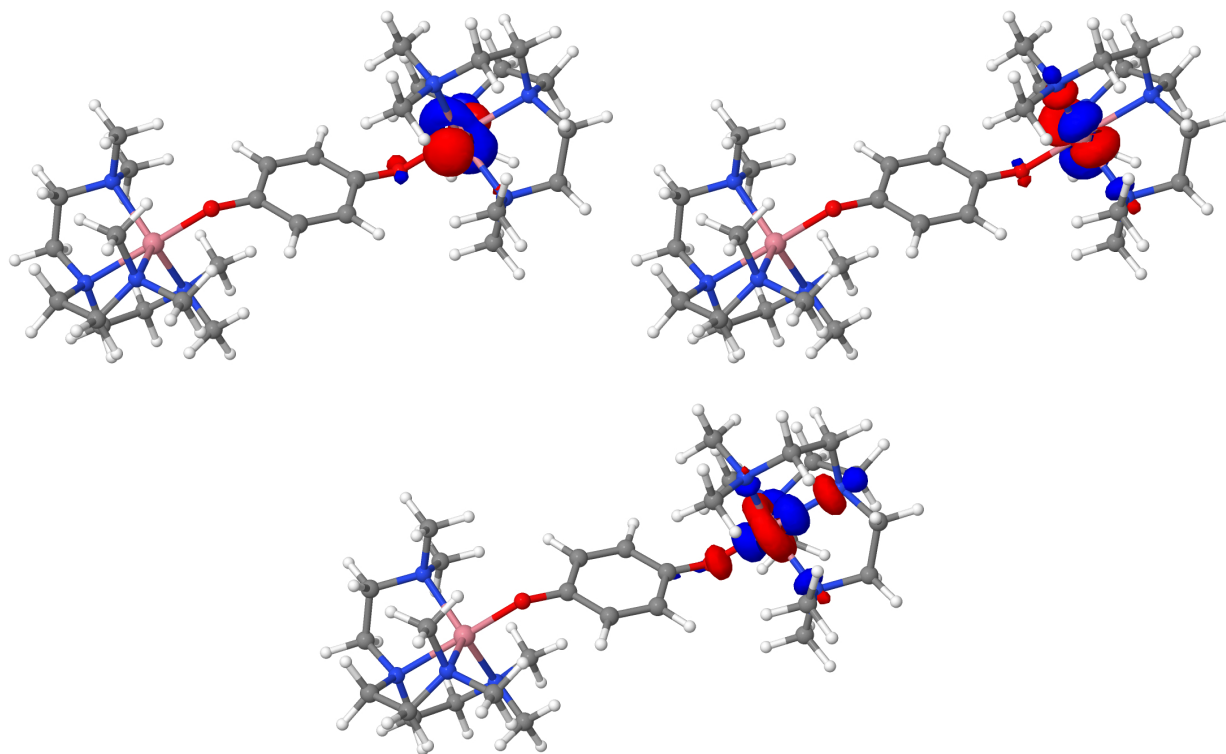
Figure S4: Isosurface of the d_{yz} (top left), d_{z^2} (top right) and $d_{x^2-y^2}$ (bottom) magnetic orbitals of **4b**. Pink = cobalt, blue = nitrogen, red = oxygen, grey = carbon, white = hydrogen. Isovalue = 0.5 a.u..
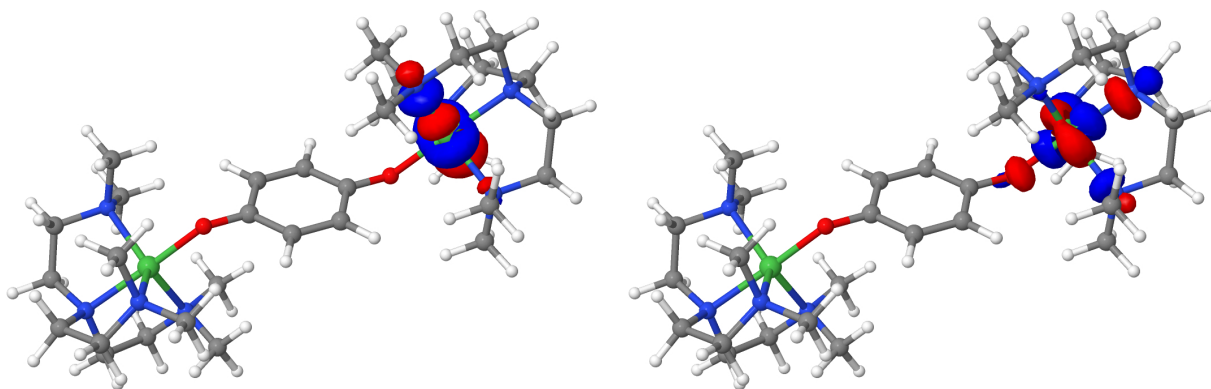

Figure S5: Isosurface of the d_{z^2} (left) and $d_{x^2-y^2}$ (right) magnetic orbitals of **5b**. Green = nickel, blue = nitrogen, red = oxygen, grey = carbon, white = hydrogen. Isovalue = 0.5 a.u..

S3 Hubbard parameters from the radical-d orbital interaction in the first and third series of compounds

Table S1: Hubbard Hamiltonian t and U parameters resulting from the radical-d orbital interaction, their energetic contribution (t^2/U), the sum of both d$\to$ rad and d$\leftarrow$ rad $(\sum t^2/U)$ and the total energetic contribution to the coupling $(-(8S_AS_B)^{-1}\sum t^2/U)$ for the first series of compounds (**1-4a**) in cm^{-1}.

		$t \times 10^{-3}$	$U \times 10^{-3}$	t^2/U	$\sum t^2/U$	ΔJ_{KE}
1a	d$_{xy} \to$ rad	-1.0	44.2	-25	-152	-843
	d$_{xy} \leftarrow$ rad	-1.4	15.3	-127		
	d$_{xz} \to$ rad	-3.1	40.0	-247	-1090	
	d$_{xz} \leftarrow$ rad	-4.5	24.4	-843		
	d$_{yz} \to$ rad	-3.3	39.6	-280	-1286	
	d$_{yz} \leftarrow$ rad	-5.1	25.4	-1006		
2a	d$_{z^2} \to$ rad	/	/	0	0	-280
	d$_{z^2} \leftarrow$ rad	/	/	0		
	d$_{xy} \to$ rad	-0.6	47.3	-7	-33	
	d$_{xy} \leftarrow$ rad	-0.8	28.2	-25		
	d$_{x^2-y^2} \to$ rad	-0.3	320.4	0	-339	
	d$_{x^2-y^2} \leftarrow$ rad	-2.9	25.6	-339		
	d$_{xz} \to$ rad	-2.2	43.1	-116	-455	
	d$_{xz} \leftarrow$ rad	-2.9	25.6	-339		
	d$_{yz} \to$ rad	-2.4	42.7	-132	-573	
	d$_{yz} \leftarrow$ rad	-3.4	27.0	-440		
3a	d$_{z^2} \to$ rad	/	/	/	-2	-314
	d$_{z^2} \leftarrow$ rad	-0.3	28.8	-3		
	d$_{x^2-y^2} \to$ rad	-0.2	40.0	-1	-2	
	d$_{x^2-y^2} \leftarrow$ rad	-0.2	31.7	-2		
	d$_{yz} \to$ rad	-2.2	54.7	-86	-489	
	d$_{yz} \leftarrow$ rad	-3.2	25.8	-403		
	d$_{xz} \to$ rad	-2.6	53.6	-128	-762	
	d$_{xz} \leftarrow$ rad	-4.1	26.9	-634		
4a	d$_{x^2-y^2} \to$ rad	/	/	0	1	-411
	d$_{x^2-y^2} \leftarrow$ rad	/	/	1		
	d$_{z^2} \to$ rad	-0.7	52.5	-10	-53	
	d$_{z^2} \leftarrow$ rad	-0.8	15.5	-43		
	d$_{yz} \leftarrow$ rad	-2.5	54.3	-113	-1181	
	d$_{yz} \to$ rad	-4.0	14.7	-1069		

8

Table S2: Hubbard Hamiltonian t and U parameters resulting from the radical-d orbital interaction, their energetic contribution (t^2/U), the sum of both d→ rad and d← rad ($\sum t^2/U$) and the total energetic contribution to the coupling ($-(8S_A S_B)^{-1} \sum t^2/U$) for the third series of compounds ($\mathbf{1c^R}$) in cm^{-1}.

		$t \times 10^{-3}$	$U \times 10^{-3}$	t^2/U	$\sum t^2/U$	ΔJ_{KE}
$\mathbf{1c^O}$	$\mathrm{d}_{xy} \to \mathrm{rad}$	-0.5	34.3	-7	17	-428
	$\mathrm{d}_{xy} \leftarrow \mathrm{rad}$	-0.6	35.3	-10		
	$\mathrm{d}_{xz} \to \mathrm{rad}$	-2.8	27.4	-285	-650	
	$\mathrm{d}_{xz} \leftarrow \mathrm{rad}$	-3.7	38.4	-365		
	$\mathrm{d}_{yz} \to \mathrm{rad}$	-2.7	28.2	-250	-618	
	$\mathrm{d}_{yz} \leftarrow \mathrm{rad}$	-3.4	30.5	-368		
$\mathbf{1c^S}$	$\mathrm{d}_{xy} \to \mathrm{rad}$	-0.5	33.7	-6	-18	-479
	$\mathrm{d}_{xy} \leftarrow \mathrm{rad}$	-0.6	31.3	-12		
	$\mathrm{d}_{yz} \to \mathrm{rad}$	-2.6	26.3	-262	-665	
	$\mathrm{d}_{yz} \leftarrow \mathrm{rad}$	-3.4	28.4	-402		
	$\mathrm{d}_{xz} \to \mathrm{rad}$	-2.7	26.3	-287	-756	
	$\mathrm{d}_{xz} \leftarrow \mathrm{rad}$	-3.6	27.8	-469		
$\mathbf{1c^{OS}}$	$\mathrm{d}_{xy}(O) \to \mathrm{rad}$	-0.6	39.2	-11	-35	-103
	$\mathrm{d}_{xy}(O) \leftarrow \mathrm{rad}$	-0.8	28.3	-25		
	$\mathrm{d}_{xz}(O) \to \mathrm{rad}$	-1.0	34.1	-32	-108	
	$\mathrm{d}_{xz}(O) \leftarrow \mathrm{rad}$	-1.4	26.2	-76		
	$\mathrm{d}_{yz}(O) \to \mathrm{rad}$	-1.3	34.7	-45	-167	
	$\mathrm{d}_{yz}(O) \leftarrow \mathrm{rad}$	-1.8	26.3	-122		
	$\mathrm{d}_{xy}(S) \to \mathrm{rad}$	-1.2	32.4	-44	-140	-767
	$\mathrm{d}_{xy}(S) \leftarrow \mathrm{rad}$	-1.5	24.4	-96		
	$\mathrm{d}_{xz}(S) \to \mathrm{rad}$	-2.4	27.0	-206	-569	
	$\mathrm{d}_{xz}(S) \leftarrow \mathrm{rad}$	-3.0	25.1	-363		
	$\mathrm{d}_{yz}(S) \to \mathrm{rad}$	-4.0	30.8	-522	-1592	
	$\mathrm{d}_{yz}(S) \leftarrow \mathrm{rad}$	-5.3	26.5	-1070		